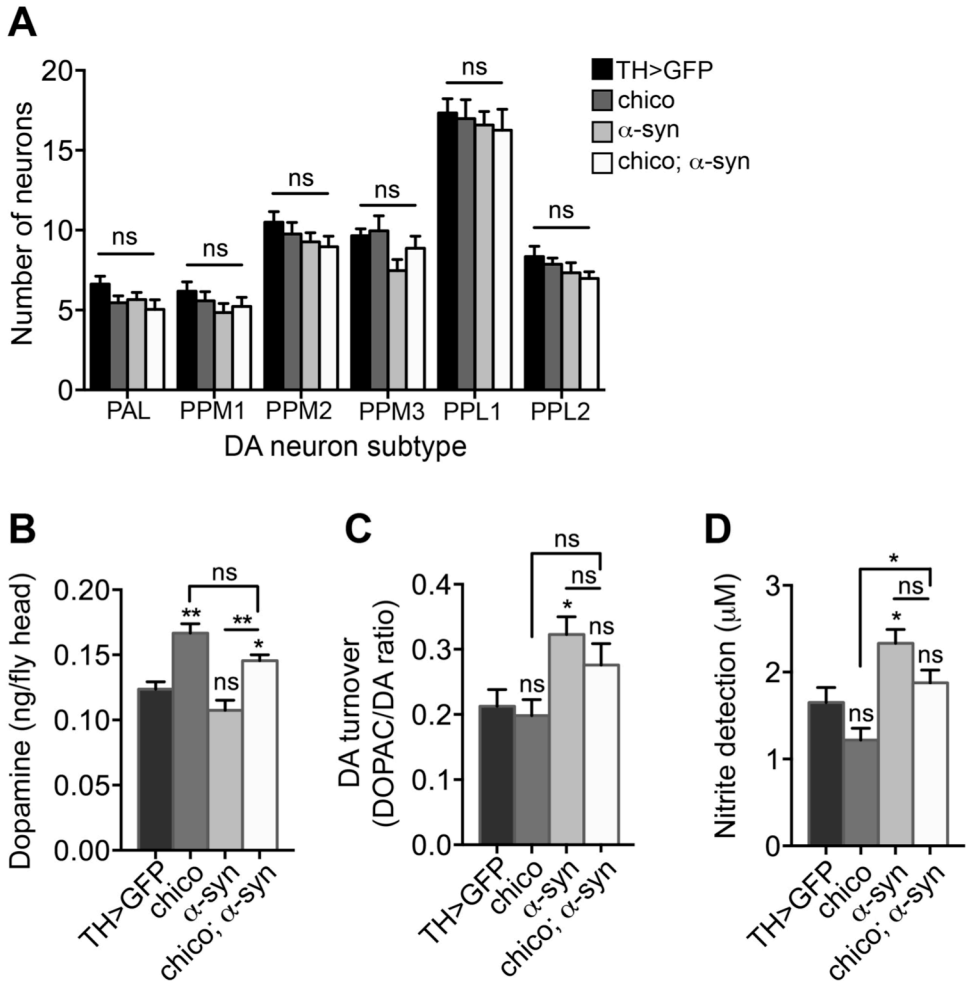

Figure S1, Related to Figure 1. *chico/IRS* mutation does not alter DA neuron numbers in newly eclosed adults. DA neurons in the brains of adult males at 24-48 hrs post-eclosion were visualized by GFP expression tyrosine hydroxylase (TH)-Gal4. **A)** Neurons were counted in each of the following DA subtype regions: anterior PAL (protocerebral anterolateral), posterior PPM1, PPM2 and PPM3 (protocerebral posterior medial), posterior PPL1 and PPL2 (protocerebral posterolateral). Values represent averages of 15 brains per genotype. **B-C)** HPLC analysis of DA and DOPAC pools in heads of male flies at 24-48 hrs post-eclosion. Values represent the average of assays from three independent head extractions and three technical replicas for each extract per genotype. Pools were quantified as ng per fly head. **D)** Nitric oxide synthase activity was determined by measuring nitrite levels secreted from dissected whole brains at 24-48 hrs post-eclosion, using a modified Griess Reagent assay. Results are displayed as μM concentration of nitrites. Values are averages of 3 replications consisting of 20-22 fly brains per replication, and three technical replicas per set of brains. Full genotypes for strains tested are: TH>GFP (*UAS-GFP/+; TH-GAL4/+*), chico (*UAS-GFP/chico; TH-GAL4/+*), α-syn (*UAS-GFP/+; TH-GAL4/UAS-α-syn*), chico; α-syn (*UAS-GFP/chico; TH-GAL4/UAS-α-syn*). Significant values are relative to *TH>GFP* controls unless otherwise indicated. Statistical analyses were performed using One-way ANOVA followed by Dunnett's post-test analysis, or Two-way ANOVA using Tukey's multiple comparisons post-test (*$p < 0.05$, ** $p < 0.01$, *** $p < 0.001$). Error bars indicate ± SEM.

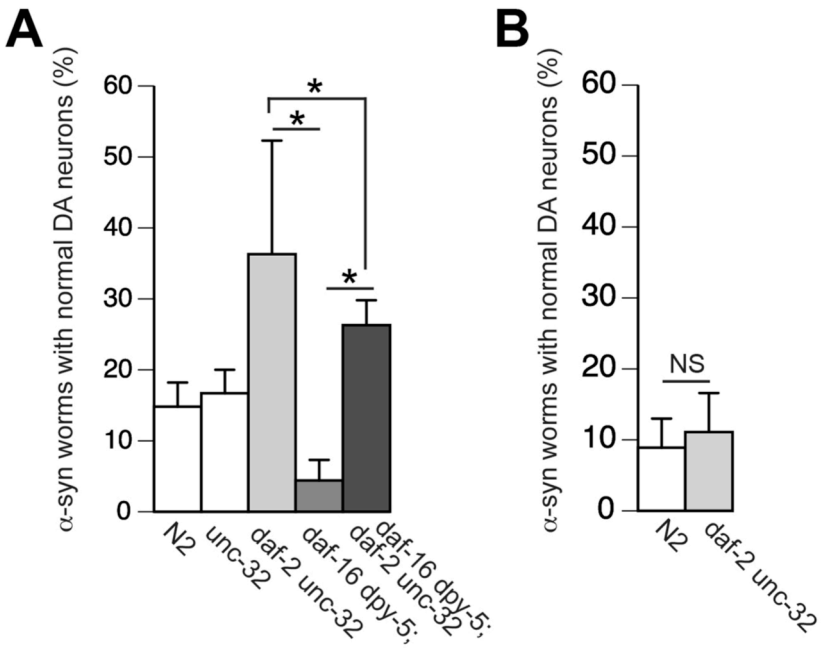

Figure S2, Related to Figure 2. The Phenotypic marker used for *daf-2* and *daf-16* is not responsible for effects of IIS pathway in DA neurons. A) IIS pathway modulates α-syn-induced DA neurodegeneration at chronological aging (day 7) in worms using different phenotypic markers *unc-32* and *dpy-5*. Similarly, *daf-2* mutation dramatically suppressed α-syn-induced DA neurodegeneration while the *daf-16* mutation enhanced α-syn-induced DA neurodegeneration. Notably, the *daf-2*; *daf-16* double mutation moderately suppressed α-syn-induced DA neurodegeneration at chronological aging. White bars indicate controls of the genetic backgrounds of the wildtype (N2), and *daf-2*mutation. **B)** The *daf-2* mutation did not suppress α-syn-induced DA neurodegeneration at biological aging (mean lifespan: day 20 for wildtype, day 40 for *daf-2* mutants). Three independent trials were performed (n=90 total), and positives were considered significant if $p<0.05$ (student's *t* test).

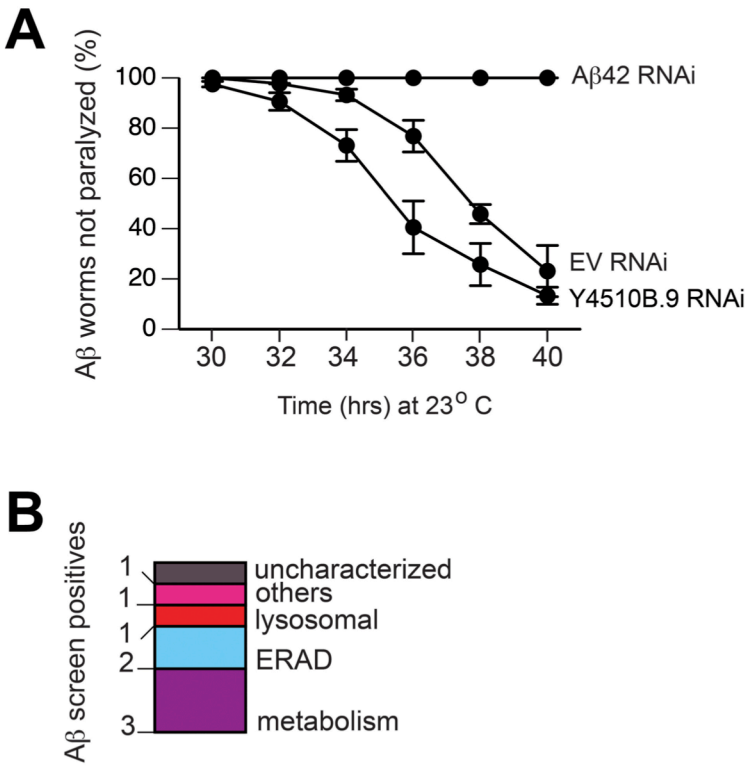

Figure S3, Related to Figure 3. Examination of positive candidates in a worm Aβ-paralysis model. **A)** Graph of Aβ-induced paralysis. Empty Vector (EV) control RNAi exhibited time-dependent paralysis phenotype. RNAi knockdown of $A\beta_{42}$ rescued paralysis, indicating that the phenotype is dependent on $A\beta_{42}$ expression. RNAi of a representative positive candidate, Y4510B.9, significantly accelerated the rate of paralysis compared to EV control. **B)** Summary of candidates that, when knocked-down, enhanced Aβ-induced paralysis. Three independent trials (n=150 total) were performed, and positives were determined as significant if $p<0.05$ (one-way ANOVA with Dunnett post-test).

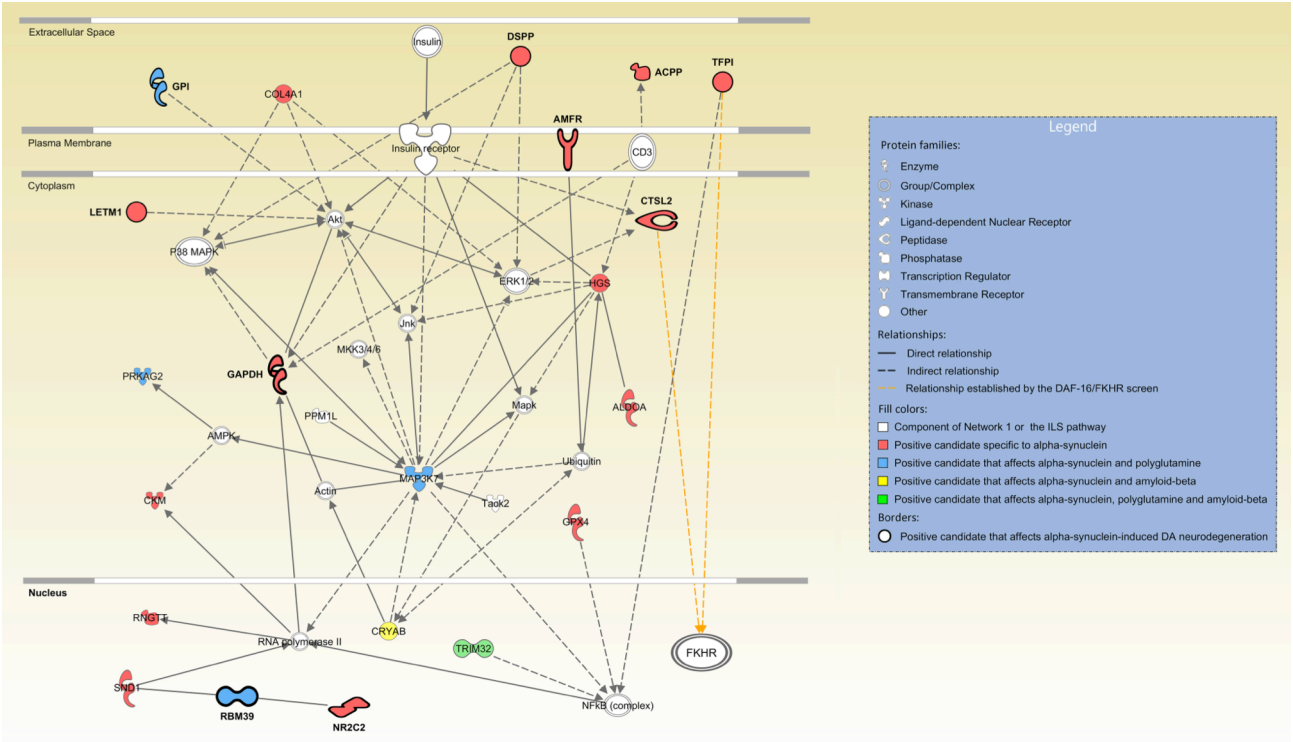

Figure S4, Related to Figure 3. Interactome network analysis of α-syn modifiers involved in energy production, nucleic acid metabolism, and small molecule biochemistry. IPA was used to assemble the most significant network (score=50, Network Table S3) based upon the interactions between α-syn modifiers and proteins associated with energy production, nucleic acid metabolism, and small molecule biochemistry. Colored proteins are α-syn modifiers identified in our primary screen; α-syn modifiers that did not affect polyglutamine or Aβ are red, α-syn modifiers that only affected polyglutamine are blue, α-syn modifiers that affected both polyglutamine and Aβ are green. Proteins that affected α-syn-induced DA neurodegeneration are highlighted by a thick border. Genes interacting directly or indirectly with α-syn modifiers are white.

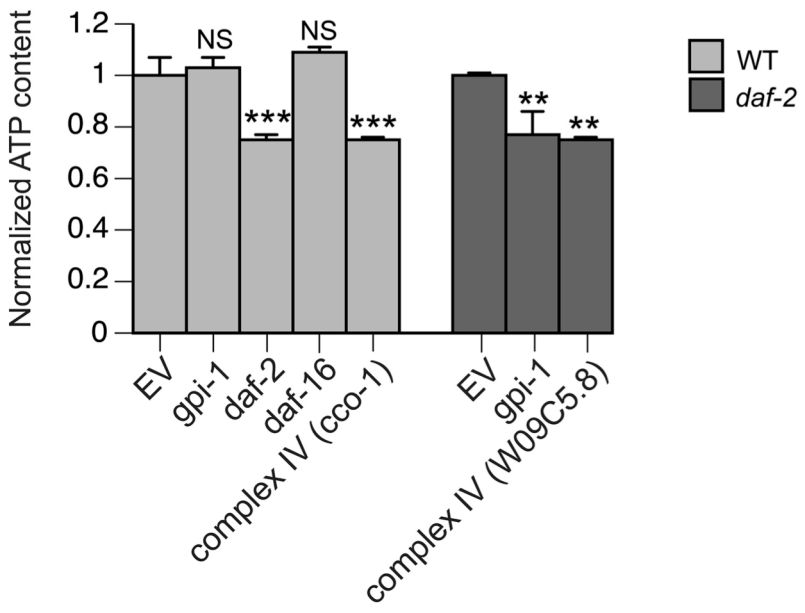

Figure S5, Related to Figure 5. The effect of *gpi-1*/GPI RNAi on ATP levels. ATP contents in both WT and *daf-2* mutant worms in the presence of P_{unc-54}::α-syn. WT or *daf-2* mutant worms were fed either EV control or RNAi bacteria expressing dsRNA against *gpi-1*, *daf-2*, *daf-16*, or genes encoding complex IV components (positive control). ATP content was measured in young adult worms using a luciferase-based assay and normalized to the ATP level in worms treated with EV RNAi bacteria of either WT or *daf-2* mutant worms. *gpi-1* RNAi had no effect on ATP production in WT worms; however it significantly reduced ATP level in *daf-2* mutant worms. In WT worms, *** is $P<0.001$; NS indicates not significant, compared with worms treated with EV control RNAi. In *daf-2* mutant worm, ** $P<0.01$, compared with worms fed with EV control RNAi bacteria. Values are mean ± SD (n = 3 independent samples with 100 worms in each). P value was calculated by one-way ANOVA with Dunnett post-test.

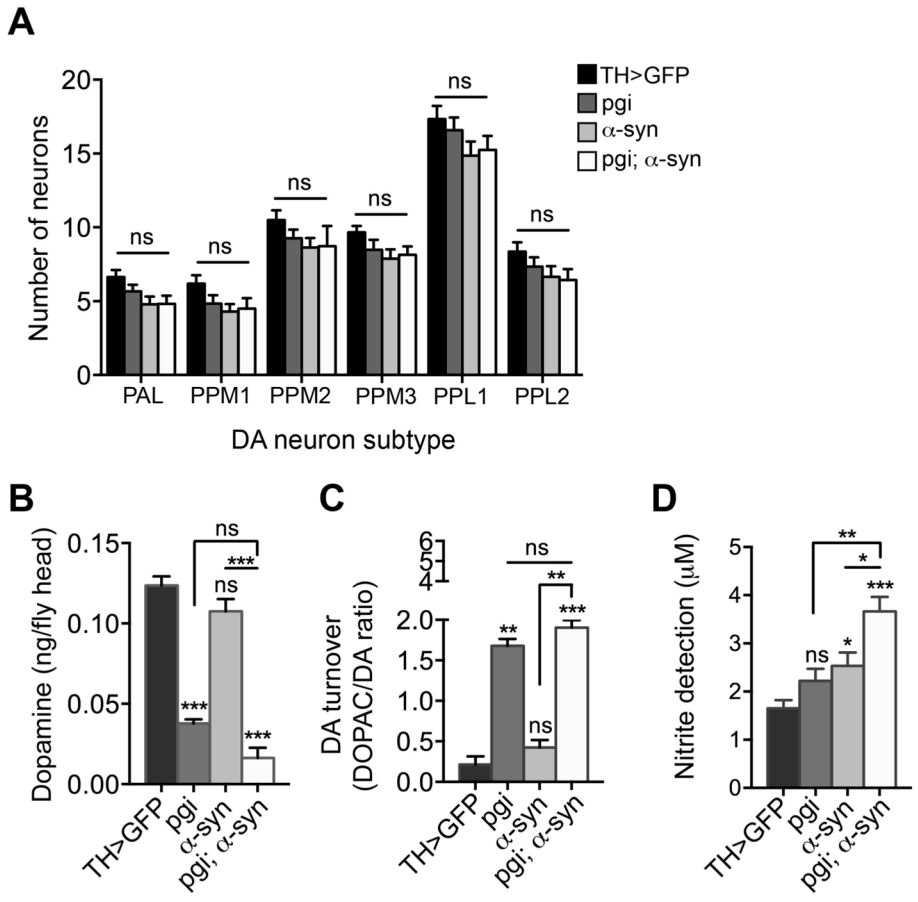

Figure S6, Related to Figure 6. *Pgi*/*GPI* mutation does not alter DA neuron numbers in newly eclosed adults. DA neurons in the brains of adult males at 24-48 hrs post-eclosion are visualized by GFP expression tyrosine hydroxylase (TH)-Gal4. **A)** Neurons were counted in each of the following dopaminergic subtype regions: anterior PAL (protocerebral anterolateral), posterior PPM1, PPM2 and PPM3 (protocerebral posterior medial), posterior PPL1 and PPL2 (protocerebral posterolateral). Values represent averages of 15 brains per genotype. **B-C)** HPLC analysis of DA and DOPAC pools in heads of male flies at 24-48 hrs post-eclosion. Values represent the average of assays from three independent head extractions and three technical replicas for each extract per genotype. Pools were quantified as ng per fly head. **D)** Nitric oxide synthase activity was determined by measuring nitrite levels secreted from dissected whole brains using a modified Griess Reagent assay. Results are displayed as μM concentration of nitrites. Values are averages of 3 replications consisting of 20-22 fly brains per replication, and three technical replicas per set of brains. Full genotypes for strains tested are: TH>GFP (*UAS-GFP/+; TH-GAL4/+*), Pgi (*UAS-GFP/Pgi; TH-GAL4/+*), α-syn (*UAS-GFP/+; TH-GAL4/UAS-α-syn*), Pgi; α-syn (*UAS-GFP/Pgi; TH-GAL4/UAS-α-syn*). To reduce experimental variability, genotypic controls and chico experimental samples shown in Figure S1 were performed simultaneously and used for analytical comparison. Significant values are relative to *TH>GFP* controls unless otherwise indicated. Statistical analyses were performed using One-way ANOVA followed by Dunnett's post-test analysis, or Two-way ANOVA using Tukey's multiple comparisons post-test (*$p < 0.05$, ** $p < 0.01$, *** $p < 0.001$). Error bars indicate ± SEM.

Movie S1. Representative video of control treatment, Related to Figure 5. Normal climbing behavior in control (TH > GFP) and experimental (TH > α-syn) flies following normal feeding. These data are associated with Figure 5F.

Movie S2. Representative video comparing the potential impact of two different food treatments in control *Drosophila*, Related to Figure 5. Control flies (TH > GFP) fed 1 M Glucose (left) or 200 mM DOG (right) were assessed via the climbing assay. These data are associated with Figure 5F.

Movie S3. Representative video comparing the effects of glucose and DOG treatment on the climbing rate of α-syn-expressing *Drosophila*, Related Figure 5. Experimental flies (TH > α-syn) fed 1M Glucose (left) or 200 mM DOG (right). These data are associated with Figure 5F.

Table S1, Related to Figure 2. Available as an Excel spreadsheet online.

Table S2, Related to Figure 2. 60 Screen positives from α-syn; *daf-2* aggregate screen and their involvement in other assays.

Gene	Brief description	DA neuron[1]	polyQ[1]	Aβ[1]	DAF-16[1]
Metabolism					
Y87G2A.8 (gpi-1)	GPI (glucose phosphate isomerase)	**	*	-	-
T07D3.7 (alg-2)	EIF2C4 (eukaryotic translation initiation factor 2C, 4)	-	-	-	-
F01F1.12 (aldo-2)	ALDOA (aldolase A, fructose-bisphosphate)	-	-	-	-
AC3.7 (ugt-1)	UGT1A6 (UDP glucuronosyltransferase 1 family, polypeptide A6)	-	-	-	-
K12G11.3 (sodh-1)	ADH4 (alcohol dehydrogenase 4 (class II), pi polypeptide)	-	-	**	-
K12G11.4 (sodh-2)	ADH1B (alcohol dehydrogenase 1B (class I), beta polypeptide)	-	-	-	**
K10B3.7 (gpd-3)	GAPDH (glyceraldehyde-3-phosphate dehydrogenase)	**	-	-	-
K10B3.8 (gpd-2)	GAPDH (glyceraldehyde-3-phosphate dehydrogenase)	*	-	-	-
ZK816.5 (dhs-26)	DHRS1 (dehydrogenase/reductase (SDR family) member 1)	-	-	-	-
C46F4.2 (acs-17)	ACSL4 (acyl-CoA synthetase long-chain family member 4)	**	-	-	*
C56G2.15	NAT6 (N-acetyltransferase 6)	**	-	-	-
Y43F8A.3	AADACL1 (neutral cholesterol ester hydrolase 1)	****	-	**	-
F25B4.1	AMT (aminomethyltransferase)	*	-	**	-
F46H5.3	CKM (creatine kinase, muscle)	-	-	-	-
F38B6.4	GART (phosphoribosylglycinamide formyltransferase, phosphoribosylglycinamide synthetase, phosphoribosylaminoimidazole synthetase)	-	-	-	-
F13D11.4	-DHL (NAD(P) dependent steroid dehydrogenase-like)	-	-	-	*
W07E11.1	DPYD (dihydropyrimidine dehydrogenase)	***	-	-	-
ERAD					
F26E4.11 (hrdl-1)	AMFR (autocrine motility factor receptor)	***	-	-	-
Y38E10A.4 (clec-8)	CSMD1 (CUB and Sushi multiple domain- 1)	*	*	-	-
T27E4.2 (hsp-16.11)	CRYAB (crystallin, alpha B)	-	-	**	-
Y45F10B.9	TRIM32 (tripartite motif-containing 32)	-	****	**	-
ER-Golgi Trafficking					
C54H2.5 (sft-4)	SURF4 (surfeit 4)	-	*	-	-
C01A2.4	CHMP2B (chromatin modifying protein 2B)	****	-	-	-
Glutathione-related					
C29E4.7 (gsto-1)	GSTO1 (glutathione S-transferase omega 1)	-	-	-	-
C54D10.2 (cdr-3)	C6orf168 (uncharacterized protein C6orf168)	-	-	-	-
T09A12.2	GPX4 (glutathione peroxidase 4)	-	-	-	-
C06A6.5	ERP44 (endoplasmic reticulum protein 44)	-	****	-	-
Glycosylation; lysosomal function					
T13B5.3 (pho-14)	ACPP (acid phosphatase, prostate)	**	-	-	-
F21F8.7 (asp-6)	CTSE (cathepsin E)	*	-	**	-
ZK550.6	PHYH (phytanoyl-CoA 2-hydroxylase)	-	-	-	-
Y71H2AR.2	CTSL2 (cathepsin L2)	*	-	-	**
T22F3.11	SLC17A5 (solute carrier family 17 (anion/sugar transporter), 5)	-	-	-	-
Signaling pathway components					
F52F12.3 (mom-4)	MAP3K7 (mitogen-activated protein kinase kinase kinase 7)	-	*	-	-
C02C2.3 (cup-4)	CHRNB1 (cholinergic receptor, nicotinic, beta 1 (muscle))	-	-	-	-
D1069.3	FAM126A (family with sequence similarity 126, member A)	**	****	-	-
R02F11.4	CEP97 (centrosomal protein 97kDa)	-	****	-	**
T01B6.3	PRKAG2 (protein kinase, AMP-activated, gamma 2 non-catalytic subunit)	-	****	-	**
Tranporters					
Y76A2A.2 (cua-1)	ATP7A (ATPase, Cu++ transporting, alpha polypeptide)	-	**	-	-
C07G1.5 (hgrs-1)	HGS (hepatocyte growth factor-regulated tyrosine kinase substrate)	-	-	-	-
Y4C6B.5	SLC46A1 (solute carrier family 46 (folate transporter), member 1)	-	**	-	-
T07G12.5	SLC23A1 (solute carrier family 23 (nucleobase transporters), member 1)	*	-	-	-
C35A5.3	SLC17A5 (solute carrier family 17 (anion/sugar transporter), member 5)	*	-	-	-
Transcription					
C03D6.3 (cel-1)	RNGTT (RNA guanylyltransferase and 5'-phosphatase)	***	-	-	-
F10G7.2 (tsn-1)	SND1 (staphylococcal nuclease and tudor domain containing 1)	-	-	-	-
F40G9.11 (mxl-2)	MLX (MAX-like protein X); Synonyms: bHLHd13, MAD7, MXD7, TCFL4	-	-	-	-

ZC395.8 (ztf-8)	DSPP (dentin sialophosphoprotein)	-	-	-	-
F44C8.3 (nhr-18)	NR2C2 (nuclear receptor subfamily 2, group C, member 2)	*	-	-	-
R03E9.1 (mdl-1)	MXI1 (MAX interactor 1)	*	-	-	-
Y55F3AM.3	RBM39 (RNA binding motif protein 39)	*	****	-	-
T05A12.4	SHPRH (SNF2 histone linker PHD RING helicase)	***	-	-	*
Others					
C24A11.8 (frm-4)	FRMD5 (FERM domain containing 5)	**	-	-	-
F01G12.5 (let-2)	COL4A1 (collagen, type IV, alpha 1)	-	-	-	*
T11F1.8		****	-	-	***
F08G2.5	DSPP (dentin sialophosphoprotein)	*	-	-	-
K10H10.5		***	-	**	-
C29F9.2	AC018737.1 (Putative uncharacterized protein E-P00000411665)	*	-	-	-
C54D10.10	TFPI (tissue factor pathway inhibitor (lipoprotein-associated coagulation inhibitor))	**	-	-	***
Uncharacterized protein					
R05F9.1	BTBD10 (BTB (POZ) domain containing 10)	*	-	**	*
W01C9.2		**	-	-	-
F35H10.7	C16orf35 (UPF0171 protein C16orf35 (Alpha-globin regulatory element-containing gene protein)(Protein CGTHBA)(-14 gene protein))	-	-	-	-

Table S3, Related to Figure S4. Functions associated with the top networks enriched for α-syn modifiers.

The 60 α-syn modifiers were analyzed through the use of IPA and were mapped to the functional networks available in the Ingenuity Pathway Knowledge Base (IPKB). Each network was comprised of a maximum of 35 interacting molecules and was given a score reflecting the chance of the α-syn modifiers falling into the network by chance alone. α-syn modifiers are shown in bold.

Molecules in Network	Genes
ACPP, Actin, Akt, **ALDOA, AMFR,** AMPK, CD3, **CKM, COL4A1, CRYAB, CTSL2, DSPP,** ERK1/2, **GAPDH, GPI, GPX4, HGS,** Jnk, **LETM1, MAP3K7,** Mapk, MKK3/4/6, NFkB (complex), NR2C2, P38 MAPK, PPM1L, **PRKAG2, RBM39,** RNA polymerase II, **RNGTT, SND1,** Taok2, **TFPI, TRIM32,**Ubiquitin	21/35
BCL6, C20orf24, CCP110, CD40LG, **CEP76,** CEP97, CEP290, **CHMP2B, CSMD1,** DEGS1, **DHRS1, DPYD, FRMD5,** GNB4, HSPB2, KIF24, LMAN1, NEURL4, **NPRL3, NSDHL, PHYH,** PIAS2, **SHPRH, SLC17A5, SLC23A1, SLC46A1, SURF4,** TAB3, TMED2, TMED7, TMED9, TMEM173, UBC, UBE2V2, UNC93B1	14/35
20-hydroxyeicosatetraenoic acid, **ACSL4, ADH4, ADH1B, AGO4, AMT,** ATOX1, **ATP7A, BTBD10,** Ca2+, **CHRNB1,** CNN2, DLG5, ERO1LB, **ERP44,** ethanol, FOS, GART, GAS1, GCSH, GLDC, GLRX, **GSTO1,** HSD17B10, KRT71, MCU, **MXI1,** MYC, **NAT6,** NUDCD1, PAM, PDZD11, UBC, UBFD1, **UGT1A6**	14/35
ACAN, AKR1B1, Aldose Reductase, ANGPT2, CaMKII, CD80, CD86, ceramide, COL2A1, **CTSE,** D-glucose, EBI3, FBXO32, FGF19, G6PD, GCH1, HSPB1, IL18, IL1B, ITPR, JINK1/2, MAP3K5, MAPK11, MAPKAPK2, miR-30c-5p (and other miRNAs w/seed GUAAACA), **MLX, NCEH1,** PLA2G4A, PRKAA, Retnlb, RNASEL, Saa3, Sapk, SELE, SPHK1	3 out of 35
APC, CTNNB1, **FAM126A**	1 out of 3

Extended Experimental Procedures

***C. elegans* Strains and Genetic Crosses**

***C. elegans* strain maintenance.** Nematodes were maintained using standard procedures (Brenner, 1974). All compound fluorescence microscopy was performed using a Nikon Eclipse E800 epifluorescence microscope equipped with Endow GFP HYQ filter cube (Chroma Technology). Images were captured with a Photometrics Cool Snap CCD camera driven by MetaMorph software (Universal Imaging).

***C. elegans* genetic crosses.** Three UA44 {*baIn11*[$P_{dat\text{-}1}$*::α-syn,* $P_{dat\text{-}1}$*::*GFP]} males and 8 DR128 [*dpy-1(e1) daf-2(e1370)*], DR129 [*daf-2(e1370) unc-32(e189)*], DR195 [*dpy-5(e61) daf-16(m26)*], or DR211 [*daf-16(m26) unc-75(e950)*] worms were transferred onto small mating plates, and incubated at 20˚C. Subsequent Dpy or Unc worm expressing GFP were analyzed for DA neurodegeneration. To generate worms for RNAi, wild type N2 (Bristol) males were crossed with DR128 [*dpy-1*(*e1*) *daf-2*(*e1370*)] to produce males with the *daf-2* mutation without Dpy phenotype. The resulting males were then crossed with UA49 {*baIn2* [$P_{unc\text{-}54}$*::*α*-syn::gfp, rol-6 (su1006)*]}, UA4 {*baIn4*[$P_{unc\text{-}54}$*::*Q82*::gfp, rol-6 (su1006)*]}, or TJ356 {*zls356*[$P_{daf\text{-}16}$*::daf-16a/b*::GFP + *rol-6(su1006)*]}, to generate strains UA134 {*baIn2*; [$P_{unc\text{-}54}$*::*α*-syn::gfp, rol-6 (su1006)*]; [*dpy-1*(*e1*) *daf-2*(*e1370*)]}, UA204 {*baIn4*[$P_{unc\text{-}54}$*::*Q82*::gfp, rol-6 (su1006)*]; [*dpy-1*(*e1*) *daf-2*(*e1370*)]}, or UA205 {*zls356*[$P_{daf\text{-}16}$*::daf-16a/b*::GFP + *rol-6*(*su1006*)]; [*dpy-1*(*e1*) *daf-2*(*e1370*)]}. The Dpy (*daf-2*), Rol (α-syn, Q82, and DAF-16), and GFP (α-syn, Q82, and DAF-16) phenotypic/fluorescent markers were used for RNAi screening.

Plasmid Constructs. Plasmids were constructed using Gateway Technology (Invitrogen; Carlsbad, CA). The cDNAs encoding *gpi-1* and *hrdl-1* were obtained from Open Biosystems (Huntsville, AL). An N-terminal FLAG tag sequence was added during the PCR amplification process. mCherry was obtained from Clontech (Mountain View, CA). The gene fusions were shuttled from entry vectors into the Gateway destination vector, pDEST-DAT-1 (Cao et al., 2005) or pDEST-UNC-54 (Hamamichi et al., 2008). The

molecular cloning yielded expression plasmids, P_{dat-1}::FLAG-*gpi-1*, P_{dat-1}::FLAG-*hrdl-1*, and P_{unc-54}::mCherry.

Generation of transgenic nematode strains. The transgenic strains, UA132 {*baIn11*[P_{dat-1}*::α-syn,* P_{dat-1}*::gfp*]; *baEx101*[P_{dat-1}*::gpi-1,* P_{unc-54}*::mCherry]*}, UA133 {*baIn11[*P_{dat-1}*::α-syn,* P_{dat-1}*::gfp*]; *baEx102*[P_{dat-1}*::hrdl-1,*P_{unc-54}*::mCherry]*} were generated by directly microinjecting 50 μg/ml expression plasmids into the integrated UA44 {*baIn11[*P_{dat-1}*::α-syn;* P_{dat-1}*::gfp]*}.

Preparation of worm protein extracts and western blotting. As described previously (Hamamichi et al., 2008), worm protein extracts were prepared and western blotting was performed to detect α-syn::GFP expression level in the *daf-2* mutant background of transgenic worms.

RNA isolation and semi-quantitative RT-PCR. As described previously (Hamamichi et al., 2008), RNA isolation and semi-quantitative RT-PCR were performed to detect α-*syn::gfp* mRNA level in the *daf-2* mutant background in transgenic worms. The following primers were designed for the PCR:

cdk-5 forward primer: 5' ggg-gat-gat-gag-ggt-gtt-cca-agc 3'

reverse primer: 5' ggc-gac-cgg-cat-ttg-aga-tct-ctg-c 3'

α-*syn* forward primer: 5' atg-gat-gta-ttc-atg-aaa-gga-ctt-tca-aag 3'

reverse primer: 5' tta-ggc-ttc-agg-ttc-gta-gtc-ttg 3'

C. elegans **RNAi screening**

RNAi screening was performed as described previously (Hamamichi et al., 2008) using RNAi feeding clones (Geneservice, Cambridge, UK) except that RNAi-treated worms were grown at 20˚C. RNAi feeding clones were grown for 14 hrs in LB culture with 100 mg/ml ampicillin and seeded onto NGM agar plates containing 1 mM isopropyl β-D-thiogalactoside. When the bacterial lawn was grown, five L4

worms were transferred onto the plates and incubated at 20˚C for 72 hrs. The gravid adults were then placed onto the corresponding RNAi plates and allowed to lay eggs for 12 hrs, and the resulting age-synchronized F1 offspring were analyzed at the proper stage for α-syn misfolding.

Analysis of α-syn misfolding. 20 young adult-staged UA134 {*baIn2*; [P_{unc-54}*::*α*-syn::gfp, rol-6 (su1006)*]; [*dpy-1*(*e1*) *daf-2*(*e1370*)]} worms were transferred onto a 2% agarose pad, immobilized with 2 mM levamisole, and scored for aggregation. The RNAi clones resulting in significant α-syn aggregation (80% of worms with increased quantity and size of aggregates) were scored as positive, and all positives were tested in triplicate.

C. elegans **Secondary screening of candidate genes from RNAi screen**

Analysis of polyglutamine aggregation. 20 L3-staged UA204 {*baInl4*[P_{unc-54}*::*Q82*::*GFP*, rol-6 (su1006)*]; [*dpy-1*(*e1*) *daf-2*(*e1370*)]} worms were transferred onto a 2% agarose pad and immobilized with 2mM levamisole, then scored in duplicate for Q82::GFP aggregation. The total number of aggregates per worm was counted, and One-way ANOVA with Dunnutt post-hoc test was used to compare the number of aggregates per worm in EV control RNAi-fed animals with candidate gene RNAi-fed animals, with $p<0.05$ considered significant.

Analysis of Aβ paralysis. Approximately 50 worms were s cored in triplicate for paralysis. The synchronized CL4176 {*smg-1*(cc546); dvIs27[pAF29(*myo-3*/Aβ_{1-42}/*let* UTR) + pRF4(*rol-6*(su1006))]} worms were kept at 16˚C for ~42 hours until all the animals reached the L3 larval stage. Paralysis of worms was scored after 28 hours Aβ induction at 23˚C when worms reached adult stage, and scoring was performed every 2 hours for the next 10-14 hours. Animals were treated with RNAi from L1 stage through the remainder of the assay. Animals were judged as paralyzed when they do not show a complete

muscle contraction in response to a prod on both their head and tail. One-way ANOVA with Dunnutt post-hoc test was used to determine significance.

Analysis of DA neurodegeneration. Thirty, six-day-old, UA197 {*sid-1 (pk3321); uIs69* [$P_{unc-119::}$*sid-1, pCFJ90* (P_{myo-2}::mCherry)]; *baIn11*[P_{dat-1}*::α-syn*, P_{dat-1}*::*GFP]} (Harrington et al., 2012) worms were transferred onto a 2% agarose pad and immobilized with 2mM levamisole, then scored in duplicate for enhanced DA neuron degeneration. For neuroprotection analysis, at least three stable lines of UA132 and UA133 were analyzed. Synchronized embryos expressing both GFP and mCherry were transferred onto NGM plates, and grown at 20˚C for 7 days. For each trial, 30 worms were transferred to a 2% agarose pad, immobilized with 2 mM levamisole, and scored. Worms were considered rescued when all four CEP and both ADE neurons were intact and had no visible signs of degeneration. Each stable line was analyzed three times (for a total of 90 worms/transgenic line). Three separate transgenic lines were analyzed per gene, for a total of 270 animals/gene analyzed. A gene candidate was deemed to be significant if $p<0.05$, one-way ANOVA with Dunnett post-test.

Analysis of DAF-16::GFP localization. Twenty, L3-staged UA205 {*zls356* [P_{daf-16}*::daf-16a/b*::GFP + *rol-6(su1006)*]; [*dpy-1*(*e1*) *daf-2*(*e1370*)]} worms were transferred onto a 2% agarose pad and immobilized with 2mM levamisole, then scored in duplicate for DAF-16::GFP localization. For each worm, GFP localization was scored as "completely nuclear", "both nuclear and cytoplasmic", or "completely cytoplasmic". It is important to note that, consistent with previous reports (Lin et al., 2001), we observed that levamisole induced constitutive nuclear localization of DAF-16::GFP within 20 minutes of immobilizing worms on the slide; to avoid this problem, we conducted all localization analyses within 8 minutes of immobilization. Two independent trials (n=40 total) were performed, and positives were determined as significant if $p<0.05$, Chi-Square test.

Temperature-sensitive (*ts*) mutant phenotype assays

The effect of *gpi-1* RNAi on *ts* mutant phenotypes was characterized in *unc-15(e1402)* and *unc-52(e669su250)* mutant worms maintained at the permissive temperature of 16^{o}C. The motility of age-synchronized N2, *unc-15* (*ts*) and *unc-52* (*ts*) were recorded at room temperature upon transferring twenty day 1 adult animals to a new 6-cm plate seeded with EV or *gpi-1* RNAi feeding bacteria. Videos of crawling worms were recorded at 7.5 frames/s, and analyzed by using WormLab3.0 (MBF Bioscience) with Kalman smoothing. The average speed of animals was calculated by dividing the total track length by the duration of each track. Each sample of 15-20 worms was measured once, and each report of motility involved three independent samples. unpaired Student's two tailed *t*-test with Welch correction.

RNA extraction, cDNA preparation and quantitative RT-PCR for DAF-16 targets

For each independent sample, total RNA was isolated from 100 late L4 to young adult hermaphrodite worms, as previously described (Hamamichi et al., 2008). The genomic DNA contamination was removed with 1 µl of DNase I (Promega) treatment for 15 min at 37°C, then with DNase Stop for 10 min at 65°C. cDNA was synthesized with iScript Reverse Transcription Supermix for RT-qPCR (Bio-Rad) following the manufacturer's protocol.

Quantitative real-time PCR reactions were performed using IQ SYBR Green Supermix (Bio-Rad) with the CFX96 Real-Time System (Bio-Rad). Each reaction contained: 7.5 µl of the IQ SYBR Green Supermix, 200 nM of forward and reverse primers and 0.3 µl of cDNA, to a final volume of 15 µl. The cycling conditions were as follows: polymerase activation and DNA denaturation at 95°C for 3 min, followed by 40 cycles of 10 s at 95°C, 30 s at 60°C. After the final cycle, a melting curve analysis was performed using the default setting of CFX96 Real-Time System. A single melt peak for each targeted gene was observed and no non-specific amplification was detected in each reaction mixture by agarose gel electrophoresis.

PCR efficiency was calculated from standard curves that were generated using serial dilutions of a cDNA pool of all worm samples (E_{sod-3}=95.7%, E_{mtl-1}=101.0%; E_{tba-1}=94.2%; E_{ama-1}=92.6%; E_{snb-1}=95.3%). The sequence of the primers is available upon request. All targeted genes were measured in duplicate and three independent biological replicates were tested for each sample. No amplification was detected in NTC and NRT controls. The Cq values recorded by CFX Manager Software version 3.0 (Bio-Rad) were exported into qBase^{PLUS} version 2.6 (Biogazelle) for determining reference target stability (GeNorm M <0.5, CV <0.2) and relative expression was normalized to three qualified reference genes, *tba-1*, *ama-1* and *snb-1*. The change of target gene expression was considered significant when P <0.05, calculated by nonparametric one-way ANOVA.

2-Deoxyglucose (DOG) analysis

Age-synchronized UA44 {*baIn11*[P_{dat-1}::*α-syn,* P_{dat-1}::GFP]} animals were grown at 20˚C, and analyzed at day 4. To minimize the effect of DOG on lifespan, 24 hrs prior to the analysis, 30 worms were transferred onto NGM plates with 5, and 10 mM DOG. These worms were then transferred to a 2% agarose pad, immobilized with 2 mM levamisole, and scored for DA neurodegeneration. The experiment was performed three times for a total of 90 worms/treatment. Statistics were performed using the one-way ANOVA with Dunnett post-hoc test.

ATP measurements

The adenosine triphosphate (ATP) assay was performed as described before (Yang et al., 2010) with minor modifications. Worms were fed with EV or *gpi-1* RNAi at 20^{o}C from embryos and worms treated with mitochondrial complex IV (*cco-1* or *W09C5.8*) RNAi were served as the positive control. 100 age-synchronized young adult worms were washed with M9 buffer, treated with three free-thaw cycles and boiled for 15 minutes to release ATP and destroy ATPase activity. Samples were then spun at 4 ^{o}C, 11,000xg for 10 minutes. A Life Technologies ATP determination kit (Molecular Probes- A22066),

which utilizes luciferase to catalyze the formation of light from ATP-dependent oxidation of D-luciferin, was used to quantify ATP contents. ATP concentrations were determined using standard curve derived from bioluminescence of known ATP concentrations. A BioTek Synergy H1 microplate reader with dispensing system was used in "well mode" such that the reagent would be dispensed to a well, delayed for 2 s, then the luminescence measured for 10s. For normalization, protein levels from the same preparation were determined by the BCA assay. Each sample was measured in duplicate and three independent samples were measured for each RNAi condition.

Drosophila strains and crosses

Drosophila strains were reared on standard molasses-based medium 23˚C. Strains used to generate transgenic control and experimental lines were: 1) Canton S, a standard wild type isogenic strain 2) *w; T(2;3)ap^{Xa} /CyO; TM6B, Tb* 3) *cn^{1} chico^{1}/CyO* [Bloomington Stock Center, stock #10738], 4)*y^{1} w^{67c23}; P{EPgy2}Pgi^{EY09730}* [Bloomington Stock Center; stock #17595], 5) *w; UAS-eGFP; TH-GAL4 (w; TH-Gal4* line was a gift from J. Hirsh, University of Virginia (Friggi-Grelin et al., 2003) and the UAS-eGFP transgene was derived from Bloomington Stock Center strain *w; P{UAS-2XEGFP}AH2* (stock #6874) 6) *w; P{UAS-Hsap\SNCA.F}5B (*expresses wild type α-syn driven by the Gal4 transcription factor and herein referred to as *UAS-α-syn*) [Bloomington Stock Center, stock # 8146]. The genotypes employed in all *Drosophila* experiments in this study were generated by standard genetic crosses and are as follows: 1) *UAS-eGFP/+; TH-GAL4/+,* 2) *UAS-GFP/Chico^{1}; TH-GAL4/+,* 3) *UAS-GFP/Pgi ^{EY0973}; TH-GAL4/+,* 4) *UAS-GFP/+; TH-GAL4/UAS-α-syn,* 5) *UAS-GFP/Chico; TH-GAL4/UAS-α-syn,* 6) *UAS-GFP/Pgi ^{EY0973}; TH-GAL4/UAS-α-syn.* Transgenic *UAS-GFP/+; TH-GAL4/+* and the wild type strain, *Canton S* served as controls in all experiments; no significant variations in assays of these two strains were observed at either 1 or 20 days post-eclosion.

DA neuron quantification

Whole brains from adult males were dissected and mounted either 24-48 hours post-eclosion or 20 days post-eclosion. DA neurons were visualized by expression of GFP under the control of the DA neuron driver TH-Gal4. Samples for quantification were imaged using a Leica TCS SP2 AOBS confocal microscope (Wetzlar, Germany). Blinded images were then analyzed using the Cell Counter plug-in in the Image J image analysis program (NIH). Results were graphed using GraphPad Prism 6 (San Diego, CA) and statistically analyzed by One-way ANOVA followed by Dunnett's post-test analysis, or Two-way ANOVA using Tukey's multiple comparisons post-test. Further details are described in the figure legends.

HPLC analysis of DA and DOPAC levels

Monoamines were separated using a CoulArray HPLC system (Model 5600; ESA, Chelmsford, MA), with a Synergi 4μm Hydro-RP column (4.6 x 150 mm; Phenomenex, Torrance, CA), modified from the method of McClung & Hirsh (1999) as described in Chaudhuri et al. (2007). Heads of adult male flies decapitated by vortexing adults flash-frozen in liquid nitrogen. Three hundred male heads were immediately homogenized in 1μl/fly head of homogenization buffer [0.1M perchloric acid] and centrifuged in 4˚C @ 9,300 x g for 10 mins. Supernatants were filtered through 0.2μm filter. The protein concentration was then determined by BioRad colorimetric protein assay, and the samples were then normalized to 25μg total protein content. Ten microliters of sample were injected for each sample and profiles were quantified by comparison to freshly prepared standards (Sigma, St. Louis, MO). All genotypes were analyzed in triplicate. Analysis was performed using ESA CoulArray software and graphed using GraphPad Prism 6 (San Diego, CA) and statistically analyzed by One-way ANOVA followed by Dunnett's post-test analysis, or Two-way ANOVA using Tukey's multiple comparisons post-test. Further details are described in the figure legends.

Griess reagent assay

Determination of nitrite levels, a quantitative assay for nitric oxide synthase activity was performed according to the method of Ajjuri & O'Donnell (2013). Briefly, the brains of male flies from all genotypes, aged to 1 or 20 days post-eclosion were dissected and immediately incubated in Grace's Insect Medium for 6 hours (Sigma, St. Louis, MO). Nitrite levels were then quantified after incubation in 1:1 ratio with Modified Griess Reagent for 5 min, after which absorbance was determined using a NanoDrop ND-1000 spectrophotometer (Thermo Scientific) at 548 nm wavelength no more than 15 min after adding Griess Reagent. Results were graphed using GraphPad Prism 6 (San Diego, CA) and statistically analyzed by One-way ANOVA followed by Dunnett's post-test analysis, or Two-way ANOVA using Tukey's multiple comparisons post-test. Further details are described in the figure legends.

***Drosophila* western blot**

Male fly heads were homogenized in RIPA lysis buffer containing 2mM dithiothreitol (DTT) and 1x protease inhibitor cocktail and run on 4-12% Bis-Tris mini gel. Proteins were transferred to Nitrocellulose Mini Membrane Transfer Stack using iBlot Gel Transfer Device. Membranes were blocked in 5% BSA in TBST. Primary antibodies anti-Dcp-1 (1:1000) and anti-syntaxin (1:500), and secondary antibodies anti-rabbit HRP (1:20,000) and anti-mouse HRP (1:20,000) were prepared in 2.5% BSA in TBST. Membranes were developed using chemiluminescence and film. Relative density was calculated using ImageJ and normalized using WT control and relative to loading controls.

Primary cortical cultures and lentiviral infections

Murine neuronal cortical cells were obtained at embryonic day 17 as described previously (Tsika et al., 2010). Lentiviral vectors containing shRNA sequences against mouse *gpi1* were obtained from Open Biosystems (# RMM3981-98071740, http://www.openbiosystems.com). Lentivirus was generated by transfection of HEK 293T cells with calcium-phosphate *N,N*-bis(2-hydroxyethyl)-2-aminoethanesulfonic

acid–DNA precipitates at 37°C with 3% CO_2 with plasmids JS86-VSV-G, CMVD82, and pLKO.1 containing the shRNA sequence. Cell culture supernatant was concentrated and viral titers were determined using a HIV-1 p24 antigen ELISA kit (Zeptometrix, www.zeptometrix.com, # 801111). Cells were seeded at 80000 cells / cm^2 and infected with lentiviral particles containing shRNA against gpi1 after 5 days in vitro (DIV) at either MOI 0.5 or 1.

Neurotoxicity analysis in primary cortical cultures

Cells were seeded in 96 well plates at 50,000 cells/well, infected at DIV 5, and fixed in 4% paraformaldehyde at the indicated time points. The staining and analysis procedures have been described in detail previously (Tsika et al., 2010). Neurotoxicity analysis was performed with 2 separate culture preparations, with 4 replicates for each preparation. One-way ANOVA with Tukey's post-hoc test was used to determine statistical significance, and $p<0.05$ was considered significant.

Sequential biochemical extraction of neuronal cultures

6,000,000 cells / condition were briefly washed in warm phosphate buffered saline followed by scraping in 200ul (10cm) of Triton X-100 lysis buffer (1% Triton X-100, 20mM HEPES pH 7.4, 150mM NaCl, 10% glycerol, 1mM EDTA, 1.5mM MgCl2, 1mM phenylmethanesulfonyl fluoride (PMSF), 50mM NaF, 2 mM Na orthovanadate, and a protease inhibitor cocktail from Roche diagnostics, www.roche.com, # 11-836-170-001). The extracts were incubated on ice for 10 minutes, subjected to 3 freeze (-80°C in ethanol) / thaw (37°C) cycles, and centrifuged at 100,000 *x g* for 30 minutes. The supernatant was saved as the Triton-soluble fraction and the pellets were extracted in 2% SDS buffer (150ml / mg of Triton X-100 soluble protein) by boiling for 20 minutes and sonication, then centrifuged at 21,000 *x g*, 22°C for 20 minutes. The supernatant was saved as the SDS-soluble fractions. Pellets were extracted in 70% formic acid by incubation at 37°C for 20 minutes, lyophilized, and resuspended in 2X sample buffer for SDS-PAGE. Samples were loaded onto NuPAGE Tris-Glycine gels (4-12%), transferred to polyvinylidene

difluoride membranes, and probed with anti-a-synuclein antibodies (syn 202, dilution 1:500, Covance, http://www.covance.com; SNL-1, dilution 1:500, gift of Benoit I. Giasson, University of Pennsylvania; or syn 505, dilution 1:500, Invitrogen, www.invitrogen.com). Anti-Neural specific enolase (NSE, Polysciences, www.polysciences.com, #16625, dilution 1:2000) and anti-alpha-tubulin (Sigma-Aldrich, www.sigma-aldrich.com, # T-6074, dilution 1:5000) were used as loading controls. Primary antibodies were detected with anti-mouse or rabbit IgG conjugated to IRDye 680 or 800 (1:10,000, LI-COR biosciences, www.licor.com). For controls, blots were scanned after the blocking step to determine autofluorescent bands, and also after the addition of secondary Ab alone. Any nonspecific bands detected were not included in densitometric analyses. Densitometric and MW analyses were performed using Odyssey Software v 2.1, LI-COR biosciences). Quantification of the Triton-soluble band migrating at 18kDa was used for monomer measurements (syn 202 and SNL-1), quantification of aggregated forms of α-synuclein was done with syn 202, SNL-1, and syn 505, and repeated with separated culture preparations. A Student's *t*-test was used to determine statistical significance; $p<0.05$ was considered significant.

Supplemental reference

Brenner, S. (1974). The genetics of *Caenorhabditis elegans*. Genetics *77*, 71-94.